



Acoustic-based estimates of Cuvier's beaked whale (*Ziphius cavirostris*) density and abundance along the U.S. West Coast from drifting hydrophone recorders

Jay Barlow¹  | Jeffrey E. Moore¹ | Jennifer L. K. McCullough²  | Emily T. Griffiths³

¹Marine Mammal and Turtle Division, Southwest Fisheries Science Center, National Marine Fisheries Service, National Oceanic and Atmospheric Administration, La Jolla, California

²Ocean Associates, Inc., under contract to Southwest Fisheries Science Center, National Marine Fisheries Service, National Oceanic and Atmospheric Administration, La Jolla, California and Cetacean Research Program, Pacific Island Fisheries Center, National Marine Fisheries Service, National Oceanic and Atmospheric Administration, Honolulu, Hawaii

³Ocean Associates, Inc., under contract to Southwest Fisheries Science Center, National Marine Fisheries Service, National Oceanic and Atmospheric Administration, La Jolla, California and Aarhus University, Department of Bioscience, Roskilde, Denmark

Correspondence

Jay Barlow, Southwest Fisheries Science Center 8901 La Jolla Shores Drive, La Jolla, CA 92037.

Email: jay.barlow@noaa.gov

Abstract

An acoustic survey of Cuvier's beaked whales (*Ziphius cavirostris*) was conducted off the U.S. West Coast in August and September 2016 using drifting recorder systems with a vertical array of two hydrophones at a depth of ~110 m. Recorders were deployed 22 times to representatively cover a 1,058,000 km² study area from the shelf break to ~556 km offshore. Vertical angles to echolocation pulses were measured using the signal time-difference-of-arrival on the two hydrophones. Echolocation pulses of Cuvier's beaked whales were identified from their arrival angles (always from below the array) and unique acoustic characteristics. The density and abundance of Cuvier's beaked whales were estimated using a group-based point-transect analysis with 2 min time snapshots. The area effectively surveyed was estimated using a maximum simulated likelihood approach to fit the observed distribution of signal arrival angles. The acoustic availability of whales during their dive cycle was estimated from the duration of acoustic encounters using a mark-recapture approach. Overall, Cuvier's beaked whales were present during 0.60% of snapshots, and their estimated average density is 5.12 animals per 1,000 km² (CV = 0.27). Their estimated abundance in the study area is 5,454 individuals (95% credibility intervals: 3,151 to 8,907).

KEYWORDS

abundance estimation, acoustic survey, Cuvier's beaked whale, drifting buoy recorder, echolocation, point-transect, vertical hydrophone array, *Ziphius cavirostris*

1 | INTRODUCTION

Population abundance and density are key elements in understanding the ecological role of a species in its ecosystem. Abundance is also important in determining the conservation status of a population and in evaluating anthropogenic threats. For cetaceans, however, abundance estimation is not trivial. Many cetaceans are distributed across entire ocean basins, making population studies difficult and expensive. Cetaceans spend much of their life submerged, which complicates the use of long-established visual sighting methods to estimate abundance. These difficulties are exemplified by Cuvier's beaked whale (*Ziphius cavirostris*), a global species with cryptic surface behavior. This species has the widest distribution of all beaked whale species, extending from the equator to high latitudes in all ocean basins (MacLeod et al., 2006). This is probably the most abundant beaked whale species, but abundance estimates exist for only a small fraction of its distribution (Barlow et al., 2006). Beaked whales are hard to see even when they are at the surface, and sighting rates decline rapidly with increasing sea state (Barlow, 2015). Cuvier's beaked whales typically forage during deep dives lasting 60–80 min and spend only 2–3 min at the surface between dives (Schorr et al., 2014), but have been documented diving for 222 min (Quick et al., 2020). For visual sighting surveys conducted from a large ship, only 40% of groups that are directly on the transect line would be detected in outstanding survey conditions (Beaufort 0 or 1) and only 13% in conditions typical of many study areas (Beaufort 4) (Barlow, 2015). The fraction detected is even smaller for aerial surveys because the potential time window for detection is much shorter (Barlow et al., 2006).

Passive acoustic survey methods, which detect cetaceans from the sounds they make, may be able to improve abundance and density estimation over visual detection methods, especially for long-diving, hard-to-see species like Cuvier's beaked whales (Barlow et al., 2021a). In many ways, Cuvier's beaked whales are ideally suited for passive acoustic surveys. Their echolocation pulses are distinctive (Baumann-Pickering et al., 2013), and 2–3 pulses are typically produced per second when foraging (Zimmer et al., 2005). The species spends approximately 20%–28% of its time foraging (Barlow et al., 2013, 2020) and forages during both day and night (Baird et al., 2008; Schorr et al., 2014). Although the echolocation beam width of Cuvier's beaked whales is estimated to be narrow (6° @ -3dB ; Zimmer et al., 2005), the pulses are very loud (up to $224\text{ dB}_{\text{pp}}$ re: $1\text{ }\mu\text{Pa}$ @ 1 m ; Gassmann et al., 2015), and on-axis pulses are estimated to be detectable at 4 km (Zimmer et al., 2008).

Cuvier's beaked whales commonly produce echolocation pulses only when they are on deep foraging dives (Warren et al., 2017). On average, echolocation begins during descent when the whales reach a depth of 462 m and continues until their ascent when they reach a depth of 881 m (Barlow et al., 2020). Based on tagging studies off southern California, foraging dives for this species last an average of 65.5 min ($SD = 6.4\text{ min}$; Barlow et al., 2020), and the mean echolocation period during these foraging dives is estimated as 39.2 min (Barlow et al., 2021a).

Previous acoustic studies of beaked whale abundance have largely been limited to Navy acoustic test facilities with a high density of seafloor hydrophones wired to the shore. Moretti et al. (2006) estimated the density of Blainville's beaked whales (*Mesoplodon densirostris*) by counting the number of groups present within a fixed time window (140 min) on an array of 82 hydrophones at the Navy's Atlantic Undersea Testing and Evaluation Center (AUTEK) in the Bahamas. They calculated group density assuming all groups would be detected once and only once during that time window. Moretti et al. (2010) developed a cue-counting method to estimate Blainville's beaked whale abundance at AUTEK using new foraging dives as cues, again assuming that all beaked whale groups (all new dives) within the hydrophone field would be detected. They used a foraging dive rate (0.36 dives/hr , $CV = 0.11$) estimated from tagged Blainville's beaked whales at AUTEK. In both studies, Moretti et al. (2010) estimated animal

density by multiplying group density by average group size (2.62, $CV = 5.5$) from visual detections of the same species in the Bahamas (Moretti et al. 2010, citing unpublished data from D. Claridge). Also, at AUTECH estimating Blainville's beaked whale density, Marques et al. (2009) used a different cue-counting approach using individual echolocation pulses as cues. They estimated the cue production rate by counting the clicking rate of individuals with acoustic recording tags. In that study, the probability of detecting a click as a function of range and orientation was estimated based on whether individual pulses (recorded on tags) were detected on nearby hydrophones. All three of these studies are dependent on having a dense array of deep hydrophones as is only found on Navy test ranges such as AUTECH, and two of the studies required cue production rates measured from tagged animals.

The methods used in these previous studies cannot be used to estimate beaked whale abundance outside of instrumented Navy ranges, which limit their utility. However, many of the general approaches developed in these studies have application elsewhere (Marques et al., 2013). Küsel et al. (2011) developed a click-based cue-counting approach in a Monte Carlo simulation framework to estimate beaked whale density with a single hydrophone using an analytical model of sound propagation to estimate detection probability as a function of range. Other studies provided the beam pattern, source level and production rate of echolocation pulses and the orientation and diving behavior of beaked whales. Although Küsel et al. (2011) also used Blainville's beaked whale at AUTECH as an example, they did not require a multiple-hydrophone array to implement that method. Hildebrand et al. (2015) estimated the density of Cuvier's and Gervais' (*Mesoplodon europaeus*) beaked whales in the Gulf of Mexico using a similar approach. These methods based on models of sound propagation require many untested assumptions about animal behavior, such as the degree to which they move their heads when searching for prey. Barlow et al. (2021a) developed three empirical methods to estimate density for Cuvier's beaked whales using drifting recorders that require fewer assumptions and outside data sources than the propagation modeling approach.

In this study, we use one of the empirical approaches of Barlow et al. (2021a) to make acoustic estimates of the density and abundance of Cuvier's beaked whales in a large study area off the U.S. West Coast. Density is estimated using a group-based, point-transect approach with "snapshot" time windows, and density estimates are extrapolated to estimate abundance in the entire study area. We analyze data collected from deployments of drifting buoy recorders with a vertical array of two-hydrophones. We identify 2 min time snapshots with beaked whale echolocation pulses. Declination angles to detected beaked whales are estimated from the time-difference-of-arrival of pulses on the two hydrophones. Applying a maximum simulated likelihood approach (Barlow et al., 2021a), these declination angles and the depth distribution of Cuvier's beaked whales (from other studies) are used to estimate range-dependent detection probability for echolocating animals. A Bayesian mark-recapture approach estimates the effective proportion of a dive cycle when groups are echolocating. Overall density is estimated from the averaged densities of individual drifts in the study area using a Bayesian approach with drifts treated as random effects. Our acoustic estimates of density are higher than prior estimates of Cuvier's beaked whale density from visual sighting surveys and are more precise.

2 | METHODS

2.1 | Field methods

Drifting buoy recorders were deployed at 22 locations offshore of the U.S. West Coast in August 2016 and were retrieved 11–23 days later (Figure 1, Table 1). In the original survey design, 19 available recorders were to be deployed at 20 locations that were approximately evenly spaced between the northern and southern U.S. Exclusive Economic Zone (EEZ) boundaries and at distances of approximately 93, 278, and 463 km (50, 150, and 250 nmi) from shore. A pilot study in 2014 showed a wide variation in drift patterns (Griffiths & Barlow, 2016), and no attempt was made to predict drift paths prior to deployments in 2016. Because only 19 recorders were available, one recorder (from drift #2) was recovered after 11 days, its data were downloaded, and it was redeployed as drift #20 (as originally planned). There were two additional, unplanned modifications to the study design. One of the original

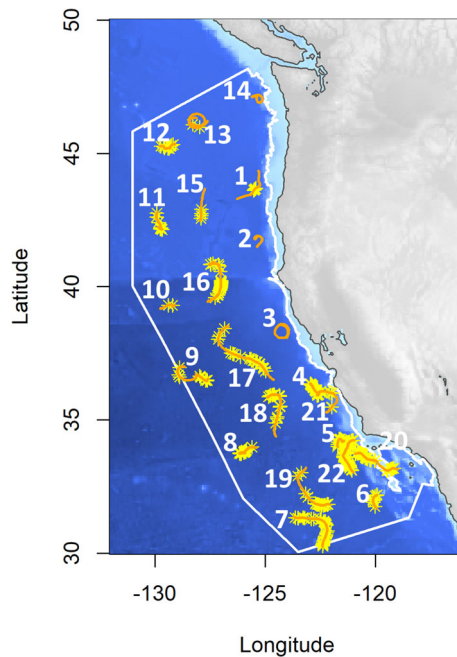


FIGURE 1 Map showing drifts of buoy recording systems (orange lines numbered 1–22) and acoustic detections of Cuvier's beaked whales (yellow asterisks). The most northeastern drift (#14) failed to record any useable data. The solid white line represents the boundary of the study area; the inshore boundary corresponds to the contiguous 500 m isobath. The 500 m isobaths around the southern Channel Islands are not shown.

19 recorders (drift #4, off the Big Sur coastline) drifted too slowly and was repositioned in similar habitat (drift #21) to give a broader geographic coverage. Another of the original 19 recorders (drift #4) was recovered after 12.8 days and redeployed (drift #22) to cover the study area more uniformly. One recorder (drift #14) failed to record any useable data, so data from only 21 drifts were available for this study.

Drifting Acoustic Spar Buoy Recorders (DASBRs) were developed at the Southwest Fisheries Science Center (Griffiths & Barlow, 2015, 2016), and the design was updated for this survey (Keating et al., 2018). All model variations included two hydrophones configured as a 10 m vertical array at a nominal depth of 100 m. Four were based on a Wildlife Acoustics (Maynard, MA) SM2+Bat recorder in a surface buoy and used conducting cable. The other 15 instruments used submersible recorders (4 Wildlife Acoustics, SM3M and 11 SoundTrap, Ocean Instruments, Auckland, New Zealand, ST4300) suspended below a surface buoy on non-conducting line. Details on each of these three systems are given in Table 2. Acoustic sampling rates were set at the maximum for 2-channel recording on each instrument, with all instruments recording 2 min files. Different duty cycles were set if necessary to obtain at least 20 days of data given the memory and battery limitations of each device. The lower hydrophone was a High Tech Inc. (Long Beach, MS) HTI-96-min in all cases and the upper hydrophone was either the same or a High Tech Inc. HTI-92-WB. All hydrophones were internally amplified with a high-pass filter at 100 Hz (SM2+Bat) or 20 Hz (SM3M and ST4300). A lower noise version of the HTI-96-min was used in all SM3M & ST4300 hydrophone arrays. A 6.8 kg (15 lb) anchor at the bottom of the array and subsurface buoys at the top of the array helped maintain a vertical orientation. A 30 m elastic cord directly below the buoy and a 30 cm dampener plate on the anchor isolated the hydrophones from movement due to waves. Array depth and tilt were measured for seven of the deployments using Loggerhead Instruments (Sarasota, FL) OpenTags, which recorded pressure and acceleration in three dimensions every 5 s. Hydrophone depths increased 5–10 m during the study due to gradual stretching of the elastic cords. Over the course of the study, the mean depth at the midpoint of the arrays was 110 m. Buoys were tracked with two Spot, LLC satellite geolocation devices (models Gen3 or Trace) in each spar buoy.

TABLE 1 Recorder type, deployment and recovery times, and drift durations for the drifts used to estimate Cuvier's beaked whale density. No useable acoustic data were recorded on drift 14.

Drift #	Recorder type	UTC deployment date and time	UTC retrieval date and time	Drift duration (days)
1	ST4300	August 20, 2016 02:07	August 31, 2016 15:04	11.5
2	ST4300	August 20, 2016 18:38	September 1, 2016 02:19	11.3
3	ST4300	August 21, 2016 10:41	September 2, 2016 16:30	12.2
4	ST4300	August 22, 2016 00:34	September 3, 2016 19:11	12.8
5	ST4300	August 22, 2016 15:05	September 4, 2016 22:51	13.3
6	ST4300	August 24, 2016 13:00	September 12, 2016 12:53	19.0
7	SM3M	August 25, 2016 09:31	September 13, 2016 09:29	19.0
8	SM2+Bat	August 26, 2016 04:56	September 14, 2016 11:39	19.3
9	ST4300	August 27, 2016 00:30	September 15, 2016 13:04	19.5
10	SM3M	August 27, 2016 17:45	September 16, 2016 04:22	19.4
11	SM2+Bat	August 28, 2016 12:47	September 17, 2016 04:18	19.6
12	ST4300	August 29, 2016 09:10	September 17, 2016 19:55	19.4
13	SM3M	August 29, 2016 20:51	September 18, 2016 04:00	19.3
14	SM2+Bat	August 30, 2016 07:51	September 18, 2016 16:08	19.3
15	ST4300	August 31, 2016 07:11	September 16, 2016 20:27	16.6
16	ST4300	September 1, 2016 13:20	September 20, 2016 23:57	19.4
17	SM3M	September 2, 2016 03:55	September 21, 2016 23:11	19.8
18	SM2+Bat	September 3, 2016 05:34	September 22, 2016 11:48	19.3
19	ST4300	September 4, 2016 11:49	September 23, 2016 06:59	18.8
20	ST4300	September 6, 2016 01:35	September 29, 2016 05:07	23.1
21	ST4300	September 4, 2016 00:05	September 25, 2016 10:03	21.4
22	ST4300	September 5, 2016 06:45	September 28, 2016 17:04	23.4
Total				397.0

TABLE 2 Characteristics of the 19 acoustic recording systems used for this study. Depth was not measured for all instruments. Hydrophone depth range represents the characteristic depths at the midpoints between the two hydrophones.

Recorder type	Number used	Sampling rate	Duty cycle on/off	Mean hydrophone depth (m)	Effective memory
SM2+Bat	4	192 kHz	2/2 min	91	1 TB
SM3M	4	256 kHz	Continuous	113	2 TB
ST4300	11	288 kHz	2/8 min	115	512 GB ^a

^aST4300 recorders had 128 GB of actual memory with $\sim 4\times$ loss-less data compression.

2.2 | Beaked whale detection

A semiautomated approach was used to detect beaked whales in the acoustic data collected on this survey. WAV files were processed using PAMGuard software (Beta version 1.15.03; Gillespie et al., 2009) to detect echolocation pulses using the Click Detector module (IIR Butterworth 4 kHz high pass filter) and to classify those pulses based on peak frequencies and the presence of a frequency change (upsweeps) based on zero crossings (see Keating & Barlow, 2013 for parameter settings). Vertical bearing angles were estimated from the time-difference-of-arrival of

the same echolocation click on the upper and lower hydrophones using the cross-correlation algorithm in PAMGuard. To identify beaked whale echolocation pulses, analysts reviewed the pulse detections (color-coded by automated peak-frequency classifications) in the time-bearing display within PAMGuard Viewer software. Potential Cuvier's beaked whale detections were initially identified independently by two experienced analysts (J.L.K.M. and E.T.G.) based on four criteria: having a downward bearing angle that remains relatively constant (varying gradually, typically by only a few degrees within a 2 min recording), a peak frequency of 32–40 kHz, secondary peaks around 18 and 23 kHz, and, frequently, an upsweep in frequency (evident in the Wigner-Ville representation of individual pulses; Barlow et al., 2021a). Surface reflections were also present for strong beaked whale signals and aided in discriminating beaked whales from dolphins, whose echolocation signals typically did not have surface reflections. All potential beaked whales were reviewed in group sessions by three of the authors (J.L.K.M., E.T.G., and J.B.). Echolocation signals from Cuvier's beaked whales were identified based on having a 32–40 kHz peak frequency, a strong null frequency at 27 kHz, secondary frequency peaks at 18–19 kHz and, or 22–24 kHz (Baumann-Pickering et al., 2013; Zimmer et al., 2005), an interpulse interval of 0.25–0.50 s (Baumann-Pickering et al., 2013), and a characteristic upsweep in the Wigner-Ville representation of the pulses. Acoustic detections of Cuvier's beaked whales were included if at least three pulses at the same bearing angle (or two pulses at the same angle and a surface reflection) had most of these characteristic features and if at least one of those pulses showed a strong upsweep in the Wigner-Ville plot. Acoustic detections were only included if all three reviewers agreed that it was a Cuvier's beaked whale. If there was any doubt about species, the detection “event” was classified as an unidentified beaked whale. After independent analyses were combined a majority (89%) of the identified Cuvier's beaked whale detections overlapped between analysts (Keating et al., 2018).

2.3 | Density estimation

The population density of Cuvier's beaked whales in the study area was estimated using a group-based, point-transect survey method with a “snapshot” sampling interval (Buckland et al., 2001, p. 173) equal to the file recording length (2 min). This sampling interval is long enough to give a high probability of detecting a group that is near the instrument, but is short enough for animal and buoy movement to be negligible and for the probability of having more than one group present within the detection range to be small. Barlow et al. (2021b) evaluated snapshot lengths of 20 s to 20 min and found that, within this range, estimates of Cuvier's beaked whale density are insensitive to the choice of snapshot length. All recorders used a 2 min file length, although the duty cycle varied among drifts. The study area was defined as the waters off the U.S. West Coast from the 500 m isobath out to approximately 556 km (300 nmi) offshore (Figure 1). This area (1,058,000 km²) corresponds to the deep-water beaked whale habitat surveyed during seven prior visual sighting surveys that produced estimates of Cuvier's beaked whale abundance (Moore & Barlow, 2017). The estimator for the density of individuals, D_i , for drift i is:

$$\hat{D}_i = \frac{F_i \cdot \hat{s}}{\hat{v} \cdot \hat{\lambda}}, \quad (1)$$

where F is the fraction of snapshot time periods with detections of Cuvier's beaked whale groups, $\hat{\lambda}$ is the estimated probability a group is available to be detected within a snapshot, \hat{v} is the estimated effective area surveyed given that a group is available, and \hat{s} is the estimated mean group size (Barlow et al., 2021a). For a given drift, F_i is equal to the number of snapshots with detections of Cuvier's beaked whale groups, n_i , divided by the total number of snapshots, k_i :

$$F_i = \frac{n_i}{k_i}. \quad (2)$$

Mean group size, $\hat{\sigma}$, was estimated to be 1.9 ($CV = 0.07$) based on 63 sightings from seven prior visual sighting surveys in the same area in 1991–2014 (Barlow, 2016). The maximum group size for Cuvier's beaked whales seen on those surveys was eight (J.B., unpublished data). The probability, $\hat{\lambda}$, that a group was acoustically active and available to be detected within a time snapshot was estimated using a new mark-recapture approach. This and the methods used to estimate effective survey area, \hat{v} , are detailed below.

2.4 | Detection angle

Point-transect distance-sampling for groups assumes that the horizontal distance from an observation point to the center of a group is unbiased. In our distance sampling approach (below), detection angles rather than detection distances were measured. In this paper we define the detection angle as the angular deviation from vertical (straight down). To help meet this assumption of unbiased distances, detection angles within a time snapshot (which may be from multiple individuals in a group) were first converted to tangents. Tangents of detection angles were averaged and back-transformed to give a mean detection angle for each snapshot.

Detection angles can be biased by refraction caused by variations in sound speed with depth. The expected bias was estimated for discrete detection angles from 5° to 85° using the Matlab (The Mathworks, Inc., Natick, MA) function *raytrace* (Val Schmidt, University of New Hampshire, 2009) based on mean sound speed profile predicted for September at the mid-point of each drift. Sound speed profiles averaged over recent decades were obtained from the *Rdata* library GOSSPL (Barlow, 2019) and interpolated at 1 m resolution. Resulting bias corrections for each drift were applied to each detection angle. Drift-specific bias corrections range from 0.01° – 0.05° (for detection angles of 5°) to 0.3° – 1.9° (for detection angles of 75°).

2.5 | Effective survey area

The effective survey area, \hat{v} , was estimated by fitting a detection function (the probability of detection as a function of range) to provide the best fit of the observed distribution of vertical detection angles to the expected distribution (Barlow et al., 2021a). The expected distribution of detection angles depends on (1) the true horizontal distribution of beaked whales (here assumed to be random with respect to a hydrophone), (2) the depth distribution of echolocating beaked whales, and (3) the probability of detection as a function of absolute distance (slant range). Half-normal (HN) and compound half-normal (C-HN) detection functions were fit using a maximum simulated likelihood approach which uses a computer simulation to estimate the expected distribution of detection angles, and which selects the detection function parameters that maximizes the likelihood of the observed distribution of detection angles (Barlow et al., 2021a). Both detection functions assume that detection is certain at zero absolute distance from the hydrophone; however, this method does not require the assumption that detection is certain at zero horizontal range. Both detection functions were fit separately for each acoustic recorder type (SM2Bat, SM3M, and ST4300) and for all recorders pooled, and the best fit model was selected based on Akaike's information criterion (AIC).

This approach (Barlow et al., 2021a) requires prior knowledge of the depth distribution of echolocation for Cuvier's beaked whales. Using information on the expected depths at which echolocation begins and ends during a foraging dive, Barlow et al. (2020) estimated the depth distribution of foraging (and presumed echolocation) for Cuvier's beaked whales that were tagged with depth-recording satellite transmitters off southern California (in the

southeastern portion of our study area). Mean foraging depths in that study were reported for different bottom-depth strata. Because virtually all of our drifts were in water depths greater than 2,000 m, we used their estimate of mean foraging depth (1,217 m, $SD = 354$ m) for that depth stratum. In distance-sampling, distant detections are typically eliminated (truncated) by excluding detections greater than a given distance (Buckland et al., 2001). In fitting the detection function, angles were truncated at 74.5° , which corresponds to a horizontal truncation distance of 4 km for a whale at this mean depth and for hydrophones at 110 m depth. After parameters were estimated for the best-fit detection function, the effective detection radius and effective survey area, \hat{v} , were estimated from the same simulation model used to estimate the detection function (Barlow et al., 2021a). Uncertainty in \hat{v} was estimated with a jackknife method. Twenty jackknife samples were created by leaving out 5% of snapshots with detections (sequentially) for each sample, reestimating the detection function parameters, and reestimating. Model selection was not repeated, and the jackknife estimates are based on the same detection function selected for the entire data set. The standard error in the estimate of \hat{v} was calculated from the jackknife estimates using standard methods (Efron, 1982).

2.6 | Acoustic availability

In order for a group within the horizontal detection range to actually be detected, it must be acoustically available. For beaked whales, acoustic availability (from Equation 1), was estimated as the expected fraction of a complete foraging-dive cycle during which a group of animals is in a vocalizing state (e.g., actively foraging) and available to be acoustically detected by a single-point hydrophone system:

$$\hat{\lambda} = \frac{T_a}{T_d}, \quad (3)$$

where T_a is the availability time and T_d is the length of a foraging dive cycle, which is the average duration between the start of successive foraging dives. We used $T_a = 191.4$ min ($SE = 28.2$ min), based on tagging studies in the southern portion of our study area (Barlow et al., 2020).

During a foraging dive, Cuvier's beaked whales produce echolocation pulses almost continuously for an average of 35 min (Warren et al., 2017). However, our recordings reveal that only short stretches of these clicking periods are actually detected. For example, for 44 dives with an initial detection distance <4 km and that were detected on continuously recording DASBRs (i.e., not duty-cycled), the mean duration from the first to last detection was about 13 min. We found no relationships between measures of acoustic availability and horizontal detection distance within this truncation distance (Figure 2). Availability time, T_a , thus measures that average stretch of time when animals are detectable to our single-point hydrophone system. This definition of availability time differs from the definition that has been used previously in the context of spatial arrays of seafloor hydrophones (Marques et al., 2013), which assumes that animals are potentially available whenever they are echolocating. The mean observed duration (e.g., 13 min in the example above) would give a low-biased estimate for because there are snapshot intervals when the animals are available but not detected (and these could occur at the beginning or end of the encounter). This low bias is exacerbated for duty-cycled DASBRs because the beginning or end of the availability time may be missed if the recorder is off. We therefore estimated with a mark-recapture analysis approach. Group detections were represented by encounter histories comprised of up to 31 2 min snapshot intervals, with the first interval representing the initial detection. Successive detections on a single drift were considered part of the same encounter history if they were within an hour from each other. A Cormack-Jolly-Seber model was used to estimate two parameters: "survival" (ϕ), which in this framework represents the probability of a group remaining available to detection during snapshot interval $t + 1$ given it was

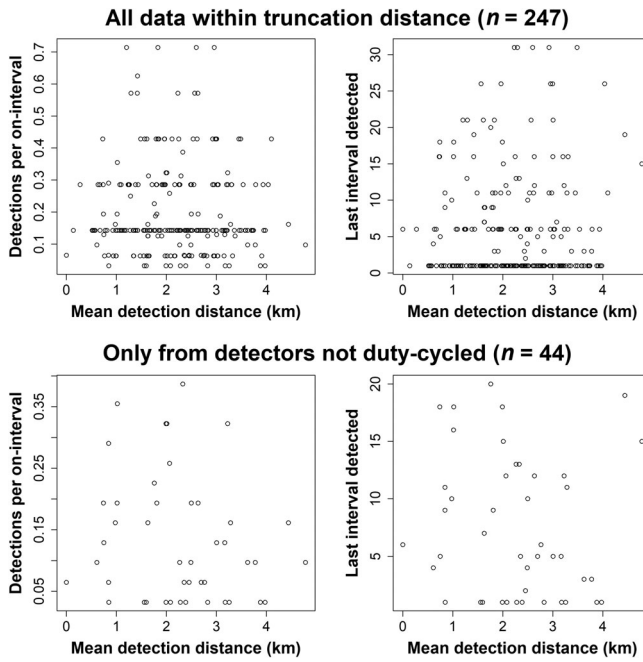


FIGURE 2 Illustrations showing the lack of relationship between horizontal detection range (x-axis) and two measures of acoustic availability. Top two panels include all data for which initial detection was within 4 km. Bottom panels are the subset of these data from detectors that were on the entire time (not duty-cycled). Left panels are a crude detection-per-effort metric (proportion of intervals out of the number of “duty cycle on-intervals” that a group was detected). Right panels are a metric of encounter duration (the last interval of detection for an encounter). Simple linear models fit to data in each panel did not reveal any statistically significant relationships between these measures ($p = .26-.74$ for the slope coefficient for detection distance). Mean detection distances are estimated from the mean of the tangent of detection angles, assuming that the whales are at the average depth of echolocation (1,217 m).

available at t , and detection probability given that it is available (p_0), which is a nuisance parameter. Both ϕ and p_0 were modeled independent of detection distance (for animals initially detected within the truncation range of 4 km; $n = 247$ encounter histories). For each interval within an encounter history j , $p_{jt} = p_0 \cdot I_{jt}$, where I_{jt} indicates whether the DASBR was recording ($I_{jt} = 1$) or not ($I_{jt} = 0$) due to duty cycling.

The “survival rate” parameter (ϕ) was used to calculate the mean “lifespan” (in terms of the number of intervals) using life table methods. This interval-lifespan, multiplied by the interval length ($x = 2$ min) to find the lifespan in minutes, and adjusted for the snapshot method by adding the interval length x (Barlow et al. 2021b), gives the snapshot availability time, T_a :

$$T_a = x \sum_{t=1}^L y(t) + x \tag{4}$$

$$y(t) = d(t) \cdot [(t - 1) + 0.5]$$

$$d(t) = \phi^{t-1} (1 - \phi).$$

Here, $d(t)$ is the marginal probability of a group becoming unavailable between the interval t and $t + 1$, and $y(t)$ is this quantity weighted by time, with representing the midpoint of interval t . Summing across all t ($L = 31$ intervals) gives the expected value for when groups “die” (become unavailable to detection).

2.7 | Density and abundance within the study area

A Bayesian MCMC approach was used to estimate population density. Substituting Equation 2 into Equation 1 and rearranging terms, the expected number of 2 min snapshots with groups detected on drift i is:

$$E[n_i] = \frac{D_i k_i \hat{\nu} \hat{\lambda}}{\hat{s}}. \quad (5)$$

The observed number of 2 min snapshot detections was treated as a Poisson random variable, i.e., $n_i \sim \text{Poisson}[E(n_i)]$. For implementation, we replaced D_i/\hat{s} with G_i (group density) and removed $\hat{\lambda}$ from the likelihood so that the posteriors for \hat{s} and $\hat{\lambda}$ are not influenced by the other parameters (these terms are brought back in at a subsequent step). Thus, the detection data were used just for estimating the density of acoustically available groups. The available-group densities for drift i were estimated as random effects, i.e., $\log(G_i) = \theta + \varepsilon_i$, where θ is the mean $\log(\text{group density})$ for the study area, and $\varepsilon_i \sim \text{Normal}(0, \sigma_G^2)$, and then $G_i = \exp[\log(G_i)]$. The mean density for the study area, \bar{D} , is the arithmetic mean of the G_i multiplied by $\hat{s}/\hat{\lambda}$, which were in the model as informed distributions (not updated by detection data). Multiplying \bar{D} by the total study area size provided an estimate of population size, N .

2.8 | MCMC specifications, priors, convergence, and goodness-of-fit

Our analysis was a multistep process, consisting of the maximum simulated likelihood estimation of $\hat{\nu}$ and two Bayesian modeling steps. The first Bayesian modeling step was fitting the mark-recapture model to the snapshot encounter histories to find the estimate of $\hat{\lambda}$. For this step, we ran two MCMC chains, each to a length of 20,000 samples including a burn-in of 5,000. Chains were thinned by two, so that posterior distributions were generated from a total of 15,000 retained samples.

The estimate of $\hat{\nu}$ and its CV, and the posterior distribution for $\hat{\lambda}$, along with ancillary estimates for \hat{s} and the detection rate data (n and k), were used as inputs to the second Bayesian modeling step, to estimate the population density parameters. For this step, we similarly ran two MCMC chains, each to a length of 1 million samples including a burn-in of 250,000 (slower mixing chains required more samples than for the mark-recapture model). Chains were thinned by five, so that posterior distributions were generated from a total of 300,000 retained samples.

For the mark-recapture model, Uniform (0,1) priors were used for ϕ and p_0 . For the population model, uninformed priors were $\theta \sim \text{Normal}(0, SD = 0.001)$ and $\sigma_G \sim \text{Uniform}(0, 4)$, while informed priors were used for group size [$s \sim \text{Normal}(1.9, SD = 0.13)$], effective survey area ($A \sim \text{Normal}$ with parameters given by the estimates from maximum simulated likelihood model), and

$\hat{\lambda}$, which was derived from the priors for dive cycle period [$T_d \sim \text{Normal}(191.4, SD = 28.2)$] and availability time ($T_a \sim \text{Normal}$ with parameters given by the posterior estimates from the Bayesian mark-recapture model).

MCMC convergence was assessed using the \hat{R} statistic, available as an output value of the function *bugs* within the R2OpenBugs package. \hat{R} was about 1.002 for ϕ and p_0 , and was less than or equal to 1.02 for all parameters in the population density model. For the population density model, the detection numbers for each drift (n_i) were compared to model expectations $[E(n_i)]$. For the mark-recapture model, the point estimates for ϕ and p_0 were used to simulate 1,000 sets of encounter histories. Each simulated set was identical to the real data with respect to sample size, the number of intervals, and duty cycling characteristics. For each simulated set, the mean number of detections per encounter history and the mean encounter duration (last interval detected) were calculated. These values for the real data set were compared to the 1,000 values for the simulated data.

TABLE 3 Number of 2 min recording snapshots, number, and percentage of snapshots with acoustic detections of Cuvier's beaked whales, model-predicted number of snapshots with detections, and estimated whale density for each drift. Note that treating drifts as random effects and the number of snapshots per drift as a random variable in a Bayesian model results in a nonzero density estimate when there were zero detections for Drifts 2 and 3.

Drift number	Number 2 min snapshots	Number snapshots with detections	% snapshots with detections	Model- predicted number snapshots	Density (individuals per 1,000 km ²)	Density CV
1	1,629	8	0.49	7.9	3.43	0.45
2	1,630	0	0.00	1.0	0.44	0.94
3	1,762	0	0.00	1.1	0.42	0.93
4	1,841	35	1.90	34.2	13.09	0.32
5	1,918	23	1.20	22.5	8.26	0.34
6	3,078	35	1.14	34.5	7.89	0.32
7	13,669	176	1.29	175.5	9.04	0.28
8	6,807	50	0.73	49.7	5.14	0.31
9	2,812	14	0.50	13.9	3.48	0.38
10	13,996	2	0.01	3.4	0.17	0.61
11	7,073	18	0.25	18.2	1.82	0.36
12	2,801	16	0.57	15.8	3.98	0.37
13	12,133	4	0.03	5.1	0.30	0.52
15	3,135	7	0.22	7.3	1.64	0.46
16	2,801	29	1.04	28.6	7.18	0.33
17	14,250	52	0.36	52.0	2.57	0.30
18	6,934	21	0.30	21.1	2.15	0.35
19	2,707	23	0.85	22.6	5.89	0.34
20	3,329	63	1.89	62.3	13.17	0.30
21	3,087	26	0.84	25.7	5.85	0.34
22	3,376	60	1.78	59.3	12.36	0.30
Overall	110,768	662	0.60	662.0	5.16	0.27

3 | RESULTS

3.1 | Data collection

Drift patterns varied widely among recording buoys (Figure 1). Excluding drift 14 (which failed to record useable data), instruments drifted for a total of 4,882 km at an average speed of 0.54 km, hr during approximately 400 days (Table 1). Duty cycle software failed on drifts 6 and 15, resulting in nearly continuous recordings for a shorter period of time (until memory was filled). Array tilts (measured with an OpenTag 3-D accelerometer on some arrays) varied during deployments but were generally $<2^\circ$. Because animals are assumed to be randomly distributed around each buoy, the mean array tilt relative to the animals is assumed to be zero. The standard deviations of the array tilt are estimated as the root-mean-squared array tilts, which were 0.42° , 0.74° , 0.75° , 0.47° , 0.68° , 0.66° , and 0.40° ($M = 0.59^\circ$), respectively for drifts 2, 5, 8, 10, 13, 16, and 20.

3.2 | Acoustic detections

PAMGuard software detected ~55 million echolocation-type signals. Of these, 85% were during night, which, based on the diurnal pattern of dolphin echolocation (Simonis et al., 2017), suggests that the vast majority of these are likely to be dolphin echolocation clicks. Beaked whales with three or more echolocation pulses were identified in 1,296 (1.17%) of the 110,767 2 min recordings used in this paper (Table 3); of these, 832 were Cuvier's beaked whales. Keating et al. (2018) present the number and geographic distribution plots for the other beaked whale detections.

The distribution of observed detection angles showed a maximum at 70°–75° and decreased sharply at greater angles (Figure 3). The number of files (2 min snapshots) with Cuvier's beaked whale detections at detection angles less than the truncation angle (74.5°) was 662 (0.60% of all snapshots); thus, truncation eliminated the most distant 20.4% of all detections. The number of files with Cuvier's beaked whales varied among the drifts from zero to 176 (Table 3). The number of echolocation pulses per sound file ranged from three (the minimum number to be considered a valid detection) to 368. There were no apparent diurnal patterns in the detection of Cuvier's beaked whale pulses.

For acoustic detections that are not truncated by detection angle, average detection durations were 17.1 min (for SM3M continuous recorders), 9.8 min (for SM2Bat duty-cycled recorders), and 12.1 min (for ST4300 duty-cycled recorders). When detections are limited to angles <74.5°, the corresponding durations were 13.3, 7.4, and 10.3 min, respectively.

3.3 | Detection function

Based on K-S test p -values, all models provided adequate fit between the observed and predicted distributions of detection angles ($p \gg .05$ for all; Table 4). However, AIC values are lower for pooled recorder types than for the sum of AIC values for recorders considered separately. Based on AIC, the best-fit model is the compound half-normal detection function with pooled recorder types (Figure 4). This best-fit model yields an effective detection radius (EDR) estimate of 3.13 km ($CV = 0.10$) and an effective area surveyed, \hat{v} , of 30.8 km² ($CV = 0.20$). The estimated value of the detection function at zero horizontal distance, $g(0)$, is 0.995.

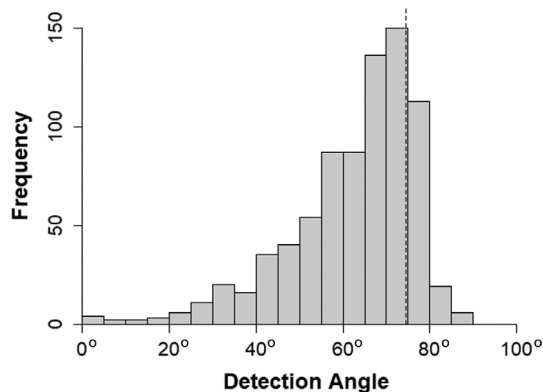


FIGURE 3 Distribution of mean detection angles for 2 min snapshot samples with three or more echolocation pulse from Cuvier's beaked whales. Angles are relative to straight down (0°). Dashed line indicates the truncation angle (74.5°) corresponding to the mean depth of echolocation for Cuvier's beaked whales at a horizontal range of 4 km.

TABLE 4 Detection function model selection values (Akaike's information criteria, AIC) for half-normal (HN) and compound half-normal (C-HN) models of snapshot detection probability as functions of absolute distance (slant range) for recorder types considered separately and pooled. Also given are Kolmogorov-Smirnov (K-S) *p*-values for the goodness of fit (between the observed and predicted distributions of detection angles) and estimates of effective detection radius (EDR) and effective area surveyed (\hat{v}).

Recorder type	Detection function	Sample size	AIC	K-S test <i>p</i> -values	EDR (km)	CV EDR	\hat{v} (km ²)	CV
ST4300	HN	339	2,539.1	.47	2.71	0.05	23.1	0.10
	C-HN	339	2,537.9	.93	3.12	0.06	30.5	0.12
SM3M	HN	234	1,755.3	.52	2.93	0.22	27.0	0.41
	C-HN	234	1,757.5	.79	2.30	0.50	16.6	0.98
SM2Bat	HN	89	658.5	.54	2.65	0.18	22.1	0.36
	C-HN	89	657.5	.91	3.15	0.13	31.1	0.25
Sum of recorders	HN	662	4,953.0					
	C-HN	662	4,952.9					
All pooled	HN	662	4,950.0	.74	2.76	0.19	24.0	0.37
	C-HN	662	4,949.0	.88	3.13	0.10	30.8	0.20

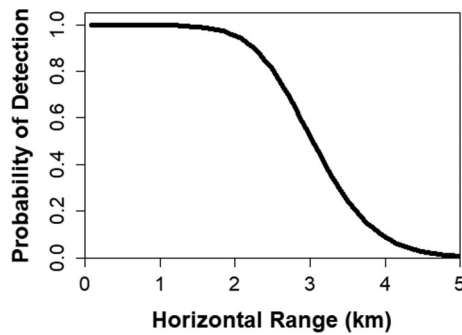


FIGURE 4 Estimated detection probabilities as a compound half-normal function of horizontal range based on the maximum simulated likelihood fit of a predicted distribution of detection angles (from a simulation) to the observed distribution (Figure 3). The estimated detection probability at zero horizontal range is .995.

3.4 | Availability time

The mark-recapture parameter estimates (posterior means) for the availability time model are $\phi = 0.892$ ($SE = 0.008$) and $p_0 = .430$ ($SE = 0.024$). Based on these estimates, groups are available for redetection for 7.615 snapshots or 15.23 min following initial detection, on average, corresponding to $T_a = 17.23$ min ($SE = 0.66$). Taken as a fraction of the dive cycle period, $\hat{\lambda} = 0.092$ ($SE = 0.015$).

3.5 | Density and abundance

Across the 21 DASBR sites with data, the posterior means for animal density (D_i) range from 0.171 to 13.1 individuals per 1,000 km² (Table 3, Figure 5). Averaging these, the overall mean density is $\bar{D} = 5.16$ animals per 1,000 km² ($SE = 1.40$, $CV = 0.27$). The total population estimate (posterior mean) is $N = 5,454$ ($SE = 1,485$, $CV = 0.27$), with a 95% Bayesian credible interval of 3,151 to 8,907. For purposes of estimating a key reference point under the U.S. Marine Mammal Protection Act, the 20th percentile of the posterior distribution for N is 4,214.

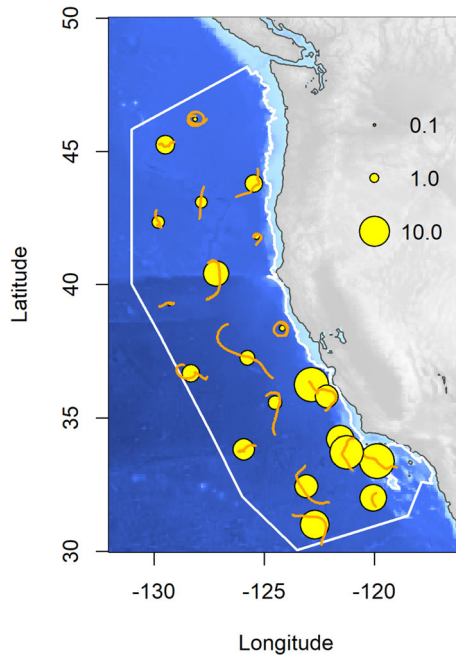


FIGURE 5 Map illustrating the geographic distribution of density estimates (whales per 1,000 km², yellow circles) for each drift (orange lines), centered at the mid-point of that drift. The area of each yellow circle is proportional to the estimated density.

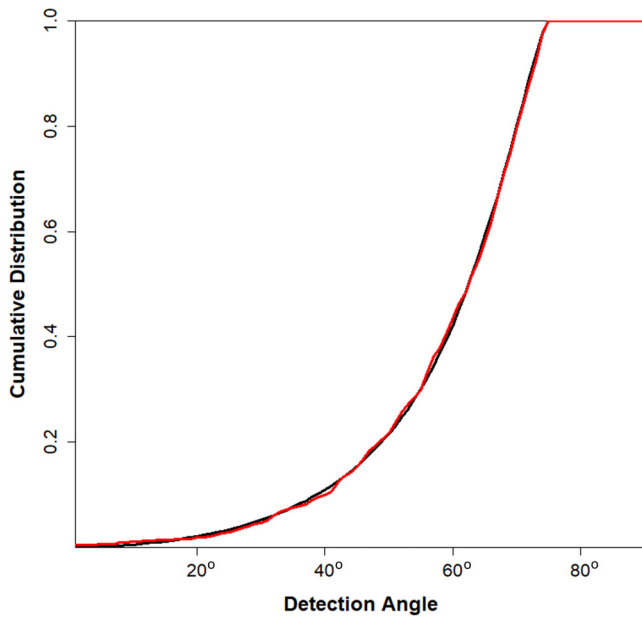


FIGURE 6 Cumulative plot showing the goodness of fit between the detection angles predicted using the best-fit detection function (Figure 3) and the simulation model (black) and the observed acoustic detection angles (red). Values are limited to angles that are less than the truncation angle (74.5°).

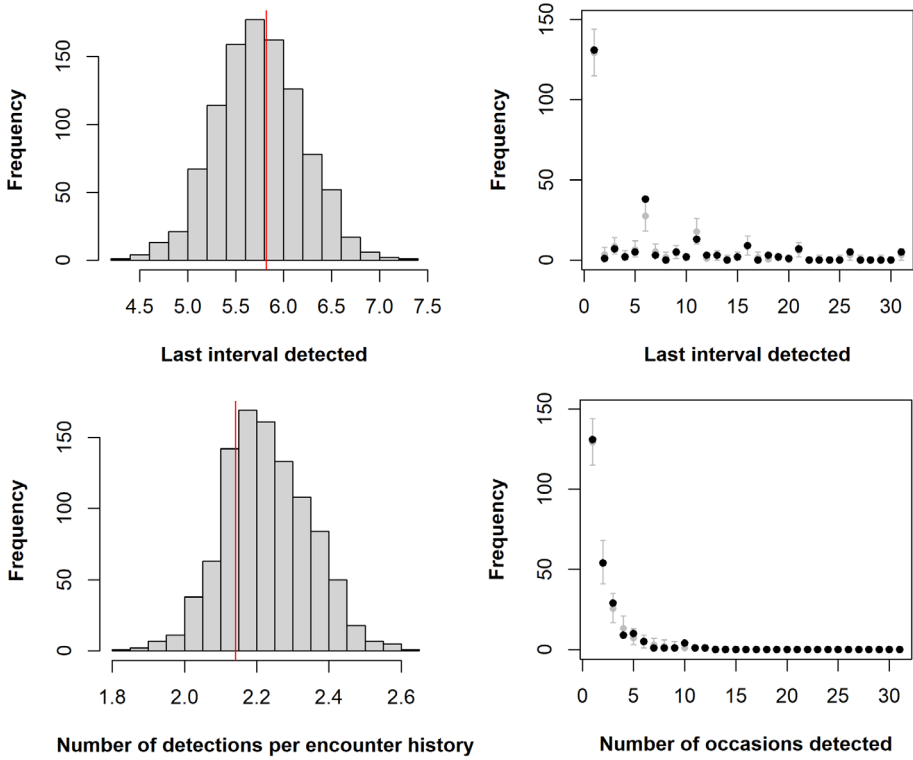


FIGURE 7 Goodness of fit plots for mark recapture analysis. Metric in top panel is encounter duration (last interval detected) and in bottom panel is the number detections per encounter history. Left panels show the real data (red line) in relation to 1,000 simulated data sets. Right panels show frequencies for real data (black dots) vs. 1,000 simulated data sets (gray bars).

3.6 | Goodness of fit

The predicted distribution of detection angles from the best-fit detection model gave a good fit to the observed distribution of detection angles (K-S test $p = .90$; Figure 6). Similarly, the Bayesian models fit the data well. For the Bayesian mark-recapture analysis, the mean number of detections and mean encounter duration for the real data set are within the middle of simulated values (Figure 7, left panels), and frequency distributions for these metrics look similar for the real and simulated data (Figure 7, right panels). For the Bayesian density analysis, the observed and expected number of detections per drift differ by a maximum of 1.4 detections ($M = 0.5$ detections) (Table 3); this makes sense given that each drift was its own random effect and suggests that the Poisson likelihood for n with normally distributed error (on log scale) was sufficient to describe variation in the n_i .

4 | DISCUSSION

4.1 | Acoustic detections

In our analyses, we assume that there are no false positive detections of Cuvier's beaked whale. We feel confident about this assumption because Cuvier's beaked whale echolocation pulses are so distinctive and of our rigorous

3-person review that required agreement by three experienced analysts. The same assumption might not be true for all beaked whale species.

The use of vertical array of two hydrophones in our study was important not only for estimating effective detection range, but also for recognizing beaked whale echolocation signals. One of the primary cues used in searching through tens of millions of echolocation signals (mostly from dolphins) was the consistency of downward bearing angles for beaked whales in the Bearing Time Display. Most dolphin echolocation clicks were received from above the horizontal plane, and all of the Cuvier's beaked whale pulses were from below. The bearing angles for beaked whale echolocation pulses typically varied little within 2-minute sound files. Although we also used an echolocation classifier which detects an upsweep (frequency change) within pulses and classifies signals by their peak frequency, these classifiers had too many false positive values to be reliable by themselves.

The geographic distribution of Cuvier's beaked whale density is clearly not uniform (Figure 1). Detections were least common in the most inshore regions in the northern portion of the study area and most common in the most inshore regions of southern California. The percentage of 2 min snapshots with acoustic detections varied widely from zero (for drifts 2 and 3) to 1.9 (for drift 4) (Table 3).

As expected, the average duration of acoustic encounters depended on the duty cycle of the recorders and the truncation angle. Duty cycled recorders have shorter acoustic encounters, likely because the recorder was not on to document the true beginning or end of the echolocation period. When detections that are greater than the truncation angle are excluded, acoustic encounters are also shorter, likely because animals moved from inside to outside this truncation angle (or vice versa) during an echolocation period.

4.2 | Detection function

The EDR for Cuvier's beaked whale echolocation pulses based on our best-fit compound half-normal model (3.13 km, $CV = 0.10$) is slightly greater than estimates from the Catalina Basin (3.00 km, Barlow et al., 2021a) and in deep basins off southern California (2.87, Barlow et al., 2021b) based on similar methods (a distance sampling approach with 1 min or 2 min snapshots). Based on other empirical estimation methods, the EDR in the Catalina Basin ranged from 2.37 km (for the spatially explicit capture-recapture method) to 2.79 km (for the trial-based method) (Barlow et al., 2021a). An alternative approach based on models of sound propagation and animal behavior produced an estimate of EDR of 2.4 km for Cuvier's beaked whales in the Gulf of Mexico (Hildebrand et al., 2015). Overall, our estimate of EDR appears to be on the high end of the range of previous estimates, although difference in truncation distance and analytical assumptions prevent a meaningful statistical comparison of these differences.

The probability of detecting a group at zero horizontal distance has been termed $g(0)$ and, in distance-sampling, is used to correct density estimates for groups that are missed. For our compound half-normal model (Figure 4), $g(0)$ is estimated to be 0.995. For the three empirical approaches to estimating EDR used by Barlow et al. (2021a), $g(0)$ estimates were similarly close to 1.0, consistent with the common distance-sampling assumption that all animals are detected at zero horizontal distance. However, the way our model is formulated, this estimate only applies to groups that are acoustically available to be detected, and although this $g(0)$ is used in estimating EDR, the much larger correction for availability bias is based on the acoustic availability time during a foraging dive (see section 4.3).

The probability of detecting an echolocating group within the 4 km truncation distance used for this analysis is estimated as 0.62 by dividing the effective area surveyed (30.8 km^2) by the area of a circle with a 4 km radius (50.3 km^2).

4.3 | Effective availability estimates

The effective snapshot availability time for the echolocation portion of a dive cycle (17.2 min) is substantially less than the expected availability time based on the predicted time spent foraging (39.2 min from Barlow et al., 2021a)

or the measured time of echolocation bouts (35 min; Warren et al., 2017). This shorter availability time is likely due to the combined effects of animal behavior and the very narrow beam angle of beaked whale echolocation pulses. At ranges greater than 700 m, whales can only be detected when their echolocation beams are pointed towards the hydrophones (Zimmer et al., 2008). Tracking studies show that foraging beaked whales change their overall direction of travel slowly during the course of a dive (Barlow et al., 2018; Gassmann et al., 2015). Given this, animals are likely to be oriented towards a hydrophone for only a portion of a foraging dive. Beaked whales are believed to move their heads up-and-down and side-to-side as they scan for potential prey items, which would increase the probability that they would be detected on a hydrophone that is ahead of them; however, an animal that is moving away from a hydrophone is unlikely to be detected until it turns.

The density estimates of Cuvier's beaked whales in the Catalina Basin (Barlow et al., 2021a) were based on an assumption that groups are acoustically available for the entire echolocation period of a foraging dive (39.2 min). Our empirical estimates indicate that true acoustic availability times are much shorter, and therefore, the density estimates of Barlow et al. (2021a) are likely to be low-biased. Barlow et al. (2021b) used an empirical mean of the mean acoustic encounter durations for continuous recordings (26.1 min). The mean acoustic encounter duration in Southern California's deep basins appears to be longer than in our larger pelagic study area.

4.4 | Abundance and density estimates

Our acoustic-based estimate of Cuvier's beaked whale abundance in the study area (5,454 animals, $CV = 0.27$) is ~50% greater than the mean abundance from seven visual sighting surveys conducted in 1991–2014 (3,645 animals, $CV = 0.35$) (Barlow 2016). This acoustic estimate falls within the range of individual estimates from these previous visual surveys (2,679–5,692) but is more precise than any of these previous surveys (CV range = 0.59–0.67) (Moore & Barlow, 2017). However, not all sources of variation are accounted for in our analyses. Specifically, our methods assume that the group size is the same as has been visually estimated during past surveys of the same area. Our estimates of precision do not include uncertainty in this assumption.

Acoustic-based density estimates were previously made for two areas within our larger study area: at the northern end of the Catalina Basin (Barlow et al., 2021a) and in three deep basins in the Southern California Bight (Barlow et al., 2021b). The mean density estimated in this study (5.16 animals per 1,000 km²) is within the range of the former (3.9–5.4 animals per 1,000 km² depending on the method used) and is much lower than the latter (31.7–36.4 animals per 1,000 km²). The higher estimates in the latter study reflect a very high density of Cuvier's beaked whale in the San Nicolas Basin (Falcone et al., 2009).

4.5 | Increasing power to detect trends in abundance

Previously, the Cuvier's beaked whale population in the study area was estimated to have decreased by approximately 2.9% per year based on visual surveys between 1991 and 2008 (Moore & Barlow, 2013). Analyses that include a new 2014 visual survey estimate indicates a possible reversal of that trend (Moore & Barlow, 2017). Both studies illustrate the difficulty in monitoring trends in Cuvier's beaked whale abundance from visual-sighting surveys with small sample sizes. Taylor et al. (2007) showed that the statistical power to detect catastrophic declines in beaked whale abundance (50% declines over 15 years) is poor for visual survey estimates. The increased precision of the acoustic estimates of abundance presented here would improve the ability to detect changes from repeated surveys. Although different potential biases make it difficult to directly compare visual and acoustic estimates and thereby extend past time series, repeated acoustic surveys hold great potential in detecting future changes in the abundance of this population. The greatest source of uncertainty in our acoustic estimates of abundance ($CV = 0.27$) comes from uncertainty in estimating the effective area surveyed ($CV = 0.20$). However, if the effective area

surveyed by one instrument does not change between surveys, trend analyses can be based on the much more precise estimates of relative abundance (from acoustic encounter rates) and much greater statistical power can be achieved in estimating trends in abundance.

4.6 | Potential biases

A fundamental assumption of our sampling is that our instrument drifts are random with respect to the distribution and abundance of the beaked whales in our study area. Although the starting locations of the drifts were under our control and were chosen to systematically cover the study area, the direction and speed of the drifts was not. If the direction and speed of the drifts is random with respect to the distribution of beaked whales, our sampling should still produce an unbiased estimate of beaked whale density. However, the passive drifting process may not be random, and DASBRs could become entrained in current systems with higher or lower densities of beaked whales than would be representative of the study area. In future studies, it would be possible to investigate this effect by testing whether beaked whale encounter rates near the starting point are statistically different from encounter rates at the end of the drift.

Another important assumption is that acoustic availability time is independent of range within our truncation angle. Although our data on availability do not show any patterns with range, there are reasons to believe that availability time could depend on range. At very close ranges, if beaked whales seldom search for prey directly above them, their echolocation beams would seldom be detected by an overhead hydrophone. This shadow effect at close range could reduce their availability time. At greater range, the fraction of time that a distant hydrophone would be at the center of their echolocation beams and be detectable should be less, which also could reduce availability time. These hypothetical effects would be difficult to observe from our data, though, since encounter histories only exist for individuals that were detected and were thus available (i.e., encounter histories provide a biased measure of true availability because the availability of undetected animals is unknown). Availability time could be modeled with a function that has a maximum at intermediate ranges.

Finally, our snapshot approach to point-transect abundance estimation assumes that animals do not move within a snapshot. If snapshot duration is short, movement is likely to be trivially small. In a tracking study within our study area, Cuvier's beaked whales were estimated to travel at an average speed of 1.2 m/s (Barlow et al., 2018). At this speed, the straight-line distance traveled in a 2 min snapshot would be 144 m, which is small compared to the EDR of 3,100 m. Simulation studies could explore the potential effect of movement on snapshot-based abundance estimation.

4.7 | Dependence on external data sources

Our estimate of abundance depends critically on two data sources that are external to our acoustic data collection: the echolocation depths of beaked whales and group size. We base our estimates of the distribution of echolocation depths from a previous tagging study that only includes the southern portion of our study area. Clearly, more information is needed on the depth distribution of echolocating Cuvier's beaked whales in our entire study area. However, Cuvier's beaked whales behave similarly in all places where they have been studied (Baird et al., 2006; Schorr et al., 2014; Tyack et al., 2006; Warren et al., 2017). Ideally, we would measure echolocation depths throughout our study area at the time of our study. Barlow & Griffiths (2017) present a method that can be used to measure both range and depth of beaked whales from a vertical hydrophone array, like we used here, but that method is severely biased if array tilt is $>0.5^\circ$, as was frequently the case in this study. To use this method on future studies, it will be important to ensure that the weights and buoys are sufficient to reduce array tilt to $<0.5^\circ$.

Our estimates of abundance also depend on external estimates of group size. In this case, however, the other studies (visual sighting surveys) were conducted within our entire study area, so there is no geographic extrapolation. Ideally, group size for acoustic estimates of abundance and density would be determined acoustically. Although beaked whales remain close enough during foraging to eavesdrop on their group members, they forage independently (Alcázar-Treviño et al., 2021). This separation between members of a group provides a potential mechanism for estimating group size acoustically. Barlow et al. (2021b) acoustically estimated a minimum group size based on the maximum number of unique bearing angles from echolocation pulses received at any time during a dive. Their estimate (1.83) is similar to the visual estimate of group size (1.9) used in this paper. Their acoustic method of estimating group size results in a biased (minimum) estimate because not all individuals are expected to be detectable simultaneously, either because they are not all facing the hydrophone or because their bearing angles are too close to be discerned. However, the similarity between visual and acoustic estimates of group size from this one study suggests that the bias may be small. The Barlow et al. (2021b) acoustic group size estimates were based on continuous recordings, and the bias associated with duty-cycled recordings is expected to be larger because there would be fewer opportunities within a dive to simultaneously detect all of the animals present. Although acoustic group size estimation is problematic, this approach may still be the most practical approach in locations where visual estimates of group size are not available.

ACKNOWLEDGMENTS

Field logistics for this acoustic survey were coordinated by Annette Henry and Shannon Rankin. We thank the officers and crew of the NOAA R/V *Bell M. Shimada* for their support and for assistance in deploying and recovering the DASBRs. Cruise leaders were Shannon Rankin, J.E.M., and J.B. Additional assistance at sea was provided by Eric Keen, Ashlyn Giddings, Bob Pitman, Karin Forney, Eric Archer, Greg Sanders, AJ Schwenger, and Colette Cairns. We thank Greg Sanders for help in funding this project. Analytical methods were developed with helpful input from Tiago Marques and Len Thomas. This manuscript benefitted from a review by Karin A. Forney.

AUTHOR CONTRIBUTIONS

Jay Barlow: Conceptualization; data curation; formal analysis; investigation; methodology; project administration; resources; software; supervision; validation; visualization; writing – original draft; writing – review and editing. **Jeffrey Moore:** Conceptualization; formal analysis; funding acquisition; investigation; methodology; project administration; resources; software; supervision; visualization; writing – original draft; writing – review and editing. **Jennifer McCullough:** Investigation; methodology; validation; writing – review and editing. **Emily Griffiths:** Investigation; methodology; validation; writing – review and editing.

ANIMAL ETHICS

All field work was conducted under a U.S. Marine Mammal Protection Act permit issued to the Southwest Fisheries Science Center and is covered under that agency's IACUC Standard Operating Procedures.

FUNDING

This study was funded in part by the National Oceanic and Atmospheric Administration (NOAA) and by the US Department of the Interior, Bureau of Ocean Energy Management through Interagency Agreement M16PG00011 with the U.S. Department of Commerce, NOAA, National Marine Fisheries Service, Southwest Fisheries Science Center. J.B. and J.E.M. were supported by the NOAA Southwest Fisheries Science Center. J.L.K.M. and E.T.G. were supported under contract to the NOAA Southwest Fisheries Science Center with funding from NOAA and the Bureau of Ocean Energy Management (BOEM).

DATA AVAILABILITY

Programs (R scripts) and associated data used to estimate the abundance of Cuvier's beaked whales are available from either of the first two authors by request.

ORCID

Jay Barlow  <https://orcid.org/0000-0001-7862-855X>

Jennifer L. K. McCullough  <https://orcid.org/0000-0003-4212-7846>

REFERENCES

- Alcázar-Treviño, J., Johnson, M., Arranz, P., Warren, V. E., Pérez-González, C. J., Marques, T., Madsen, P. T., & Aguilar de Soto, N. (2021). Deep-diving beaked whales dive together but forage apart. *Proceedings of the Royal Society B: Biological Sciences*, 288(1942), 20201905. <https://doi.org/10.1098/rspb.2020.1905>
- Baird, R. W., Webster, D. L., McSweeney, D. J., Ligon, A. D., Schorr, G. S., & Barlow, J. (2006). Diving behaviour and ecology of Cuvier's (*Ziphius cavirostris*) and Blainville's beaked whales (*Mesoplodon densirostris*) in Hawai'i. *Canadian Journal of Zoology*, 84, 1120–1128.
- Baird, R. W., Webster, D. L., Schorr, G. S., McSweeney, D. J., & Barlow, J. (2008). Diel variation in beaked whale diving behavior. *Marine Mammal Science*, 24(3), 630–642. <https://doi.org/10.1111/j.1748-7692.2008.00211.x>
- Barlow, J. (2015). Inferring trackline detection probabilities, $g(0)$, for cetaceans from apparent densities in different survey conditions. *Marine Mammal Science*, 31(3), 923–943. <https://doi.org/10.1111/mms.12205>
- Barlow, J. (2016). *Cetacean abundance in the California Current estimated from ship-based line-transect surveys in 1991–2014*. Southwest Fisheries Science Center Administrative Report LJ-16-01.
- Barlow, J. (2019). *Global Ocean Sound Speed Profile Library (GOSSPL), an Rdata resource for studies of ocean sound propagation* (NOAA Technical Memorandum NOAA-TM-NMFS-SWFSC-612). U. S. Department of Commerce.
- Barlow, J., Ferguson, M., Perrin, W. F., Ballance, L., Gerrodette, T., Joyce, G., MacLeod, C. D., Mullin, K., Palka, D. L., & Waring, G. (2006). Abundance and density of beaked and bottlenose whales (family Ziphiidae). *Journal of Cetacean Research and Management*, 7(3), 263–270.
- Barlow, J., Fregosi, S., Thomas, L., Harris, D., & Griffiths, E. T. (2021a). Acoustic detection range and population density of Cuvier's beaked whales estimated from near-surface hydrophones. *Journal of the Acoustical Society of America*, 149(1), 111–125. <https://doi.org/10.1121/10.0002881>
- Barlow, J., & Griffiths, E. T. (2017). Precision and bias in estimating detection distances for beaked whale echolocation clicks using a two-element vertical hydrophone array. *Journal of the Acoustical Society of America*, 141(6), 4388–4397. <https://doi.org/10.1121/1.4985109>
- Barlow, J., Trickey, J. S., Schorr, G. S., & Moore, J. E. (2021b). Recommended snapshot length for acoustic point-transect surveys of intermittently available beaked whales. *Journal of the Acoustical Society of America*, 149, 3830–3840. <https://doi.org/10.1121/10.0005108>
- Barlow, J., Griffiths, E. T., Klinck, H., & Harris, D. (2018). Diving behavior of Cuvier's beaked whales inferred from three-dimensional acoustic localization and tracking using a nested array of drifting hydrophone recorders. *Journal of the Acoustical Society of America*, 144, 2030–2041. <https://doi.org/10.1121/1.5055216>
- Barlow, J., Schorr, G. S., Falcone, E. A., & Moretti, D. J. (2020). Variation in dive behavior of Cuvier's beaked whales with sea-floor depth, time-of-day, and lunar illumination. *Marine Ecology Progress Series*, 644, 199–214. <https://doi.org/10.3354/meps13350>
- Barlow, J., Tyack, P. L., Johnson, M. P., Baird, R. W., Schorr, G. S., Andrews, R. D., & N. Aguilar de Soto. (2013). Detection probabilities for acoustic surveys of Cuvier's and Blainville's beaked whales. *Journal of the Acoustical Society of America*, 134(3), 2486–2496. <https://doi.org/10.1121/1.4816573>
- Baumann-Pickering, S., McDonald, M. A., Simonis, A. E., Solsona Berga, A., Merckens, K. P., Oleson, E. M., Roch, M. A., Wiggins, S. M., Rankin, S., Yack, T. M., & Hildebrand, J. A. (2013). Species-specific beaked whale echolocation signals. *Journal of the Acoustical Society of America*, 134(3), 2293–2301. <https://doi.org/10.1121/1.4817832>
- Buckland, S. T., Anderson, D. R., Burnham, K. P., Laake, J. L., Borchers, D. L., & Thomas, L. (2001). *Introduction to Distance Sampling: Estimating abundance of biological populations*. Oxford University Press.
- Efron, B. (1982). *The jackknife, the bootstrap and other resampling plans*. Society for Industrial and Applied Mathematics.
- Falcone, E., Schorr, G.S., Douglas, A., Calambokidis, J., Henderson, E., McKenna, M., Hildebrand, J., & Moretti, D (2009). Sighting characteristics and photo-identification of Cuvier's beaked whales (*Ziphius cavirostris*) near San Clemente Island, California: a key area for beaked whales and the military? *Marine Biology*, 156, 2631–2640. <https://doi.org/10.1007/s00227-009-1289-8>
- Gassmann, M., Wiggins, S. M., & Hildebrand, J. A. (2015). Three-dimensional tracking of Cuvier's beaked whales' echolocation sounds using nested hydrophone arrays. *Journal of the Acoustical Society of America*, 138, 2483–2494. <https://doi.org/10.1121/1.4927417>
- Gillespie, D., Mellinger, D. K., Gordon, J., McLaren, D., Redmond, P., McHugh, R., Trinder, P., Deng, X. Y., & Thode, A. (2009). PAMGUARD: Semiautomated, open source software for real-time acoustic detection and localization of cetaceans. *Journal of the Acoustical Society of America*, 125(4), 2547–2547. <https://doi.org/10.1121/1.4808713>

- Griffiths, E. T., & Barlow, J. (2015). *Equipment performance report for the drifting acoustic spar buoy recorder (DASBR)* (NOAA Technical Memorandum NOAA-TM-NMFS-SWFSC-543). U. S. Department of Commerce.
- Griffiths, E. T., & Barlow, J. (2016). Cetacean acoustic detections from free-floating vertical hydrophone arrays in the southern California Current. *Journal of the Acoustical Society of America*, 140(5), EL399–EL404. <https://doi.org/10.1121/1.4967012>
- Hildebrand, J. A., Baumann-Pickering, S., Frasier, K. E., Trickey, J. S., Merckens, K. P., Wiggins, S. M., McDonald, M. A., Garrison, L. P., Harris, D., Marques, T. A., & Thomas, L. (2015). Passive acoustic monitoring of beaked whale densities in the Gulf of Mexico. *Scientific Reports*, 5, 16343. <https://doi.org/10.1038/srep16343>
- Keating, J. L., & Barlow, J. (2013). *Click detectors and classifiers used during the 2012 southern California behavioral response study* (NOAA Technical Memorandum NOAA-TM-NMFS-SWFSC-517). U.S. Department of Commerce.
- Keating, J. L., Barlow, J., Griffiths, E. T., & Moore, J. E. (2018). *Passive acoustics survey of cetacean abundance levels (PASCAL-2016) final report*. U.S. Department of the Interior, Bureau of Ocean Energy Management. OCS Study BOEM 2018-025.
- Küsel, E.T., Mellinger, D.K., Thomas, L., Marques, T.A., Moretti, D. J., & Ward, J. (2011). Cetacean population density estimation from single fixed sensors using passive acoustics. *Journal of the Acoustical Society of America*, 129(6), 3610–3622. <https://doi.org/10.1121/1.3583504>
- MacLeod, C., Perrin, W. F., Pitman, R., Barlow, J., Ballance, L., D'Amico, A., Gerrodette, T., Joyce, G., Mullin, K. D., Palka, D. L., & Waring, G. T. (2006). Known and inferred distributions of beaked whale species (Cetacean: Ziphiidae). *Journal of Cetacean Research and Management*, 7(3), 271–286.
- Marques, T. A., Thomas, L., Martin, S. W., Mellinger, D. K., Wards, J. A., Moretti, D. J., Harris, D., & Tyack, P. L. (2013). Estimating animal population density using passive acoustics. *Biological Reviews*, 88(2), 287–309. <https://doi.org/10.1111/brv.12001>
- Marques, T. A., Thomas, L., Ward, J., DiMarzio, N., & Tyack, P. L. (2009). Estimating cetacean population density using xed passive acoustic sensors: an example with Blainville's beaked whales. *Journal of the Acoustical Society of America*, 125, 1982–1994. <https://doi.org/10.1121/1.3089590>
- Moore, J. E., & Barlow, J. (2013). Declining abundance of beaked whales (Family Ziphiidae) in the California Current Large Marine Ecosystem. *PLoS ONE*, 8(1), e52770. <https://doi.org/10.1371/journal.pone.0052770>
- Moore, J., & Barlow, J. (2017). *Population abundance and trend estimates for beaked whales and sperm whales in the California Current from ship-based visual line-transect survey data, 1991 - 2014* (NOAA Technical Memorandum NOAA-TM-NMFS-SWFSC-585). U.S. Department of Commerce.
- Moretti, D., DiMarzio, N., Morrissey, R., Ward, J., & Jarvis, S. (2006). Estimating the density of Blainville's beaked whale (*Mesoplodon densirostris*) in the Tongue of the Ocean (TOTO) using passive acoustics. *Proceedings of the Oceans'06 MTS, IEEE*, Boston, MA.
- Moretti, D., Marques, T. A., Thomas, L., DiMarzio, N., Dille, A., Morrissey, R., McCarthy, E., Ward, J., & Jarvis, J. (2010). A dive counting density estimation method for Blainville's beaked whale (*Mesoplodon densirostris*) using a bottom-mounted hydrophone field as applied to a Mid-Frequency Active (MFA) sonar operation. *Applied Acoustics*, 71(11), 1036–1042. <https://doi.org/10.1016/j.apacoust.2010.04.011>
- Quick, N. J., Cioffi, W. R., Shearer, J. M., Fahlman, A., & Read, A. J. (2020). Extreme diving in mammals: first estimates of behavioural aerobic dive limits in Cuvier's beaked whales. *Journal of Experimental Biology*, 223(18), jeb222109. <https://doi.org/10.1242/jeb.222109>
- Simonis, A. E., Roch, M. A., Bailey, B., Barlow, J., Clemesha, R. E., Iacobellis, S., Hildebrand, J. A., & Baumann-Pickering, S., 2017. Lunar cycles affect common dolphin *Delphinus delphis* foraging in the Southern California Bight. *Marine Ecology Progress Series*, 577, 221–235. <https://doi.org/10.3354/meps12247>
- Schorr, G. S., Falcone, E. A., Moretti, D. J., & Andrews, R. D. (2014). First long-term behavioral records from Cuvier's beaked whales (*Ziphius cavirostris*) reveal record-breaking dives. *PLoS ONE*, 9(3), e92633. <https://doi.org/10.1371/journal.pone.0092633>
- Taylor, B. L., Martinez, M., Gerrodette, T., Barlow, J., & Hrovat, Y. N. (2007). Lessons from monitoring trends in abundance of marine mammals. *Marine Mammal Science*, 23(1), 157–175. <https://doi.org/10.1111/j.1748-7692.2006.00092.x>
- Tyack, P. L., Johnson, M., Aguilar Soto, N., Sturlese, A., & Madsen, P. T. (2006). Extreme diving of beaked whales. *Journal of Experimental Biology*, 209(21), 4238–4253. <https://doi.org/10.1242/jeb.02505>
- Warren, V. E., Marques, T. A., Harris, D., Thomas, L., Tyack, P. L., Aguilar de Soto, N., Hickmott, L. S., & Johnson, M. P. (2017). Spatiotemporal variation in click production rates of beaked whales: Implications for passive acoustic density estimation. *Journal of the Acoustical Society of America*, 141, 1962–1974. <https://doi.org/10.1121/1.4978439>
- Zimmer, W. M. X., Harwood, J., Tyack, P. L., Johnson, M. P., & Madsen, P. T. (2008). Passive acoustic detection of deep-diving beaked whales. *Journal of the Acoustical Society of America*, 124(5), 2823–2832. <https://doi.org/10.1121/1.2988277>
- Zimmer, W. M. X., Johnson, M. P., Madsen, P. T., & Tyack, P. L. (2005). Echolocation clicks of Cuvier's beaked whales (*Ziphius cavirostris*). *Journal of the Acoustical Society of America*, 117(6), 3919–3927. <https://doi.org/10.1121/1.1910225>

How to cite this article: Barlow, J., Moore, J. E., McCullough, J. L. K., & Griffiths, E. T. (2022). Acoustic-based estimates of Cuvier's beaked whale (*Ziphius cavirostris*) density and abundance along the U.S. West Coast from drifting hydrophone recorders. *Marine Mammal Science*, 38(2), 517–538. <https://doi.org/10.1111/mms.12872>